

ILGAR-In<sub>2</sub>S<sub>3</sub> buffer layers for Cd-free Cu(In, Ga)(S, Se)<sub>2</sub> solar cells with certified efficiencies above 16%

R. Sáez-Araoz, J. Krammer, S. Harndt, T. Koehler, M. Krueger, P. Pistor, F. Hergert, A. Jasenek, M. Ch. Lux-Steiner, Ch. –H. Fischer

## ABSTRACT

In<sub>2</sub>S<sub>3</sub> buffer layers have been prepared using the spray ILGAR (ion layer gas reaction) deposition technique for chalcopyrite-based thin-film solar cells. These buffers deposited on commercially available Cu(In, Ga)(S, Se)<sub>2</sub> absorbers have resulted in solar cells with certified record efficiencies of 16.1%, clearly higher than the corresponding CdS-buffered references. The deposition process has been optimized and the resulting cells have been studied using current-voltage and quantum efficiency analysis, and compared with previous record cells, cells with a thermally evaporated In<sub>2</sub>S<sub>3</sub> buffer layer and CdS references.

## INTRODUCTION

Chalcopyrite-based thin film photovoltaics is already regarded as an alternative to Si-based technology. Recently, laboratory-scale Cu(In, Ga)Se<sub>2</sub> solar cells have surpassed the remarkable barrier of 20 % [1]. At the industrial level, the efficiency figures are also steadily raising [2,3]. In both cases, the devices usually include a CdS buffer layer deposited in a chemical bath (CBD), which shows various disadvantages: not only is the material toxic, but also the deposition method is not well suited for in-line processing.

During the last years there have been many attempts to tackle these issues [4]. Dry or quasi-dry processes capable of depositing non-toxic materials for buffer layers include physical vapor deposition (PVD) [5], sputtering [6], atomic layer deposition (ALD)[7] and the Spray-Ion Layer Gas Reaction (Spray-ILGAR) [8], which has been recently awarded the title German High Tech Champion 2011 in the field of photovoltaics by the Fraunhofer Gesellschaft ([www.research-in-germany.de/ghtc](http://www.research-in-germany.de/ghtc)). Spray-ILGAR In<sub>2</sub>S<sub>3</sub> has already shown its feasibility for replacing CdS buffer layers in commercially available Cu(In, Ga)(S, Se)<sub>2</sub> (CIGSSe) absorbers with a certified efficiency of 14.7 % [9]. With evaporated-In<sub>2</sub>S<sub>3</sub> the certified efficiency on laboratory-based absorbers has reached 15.2 % [10], while 16.6% efficiency has been recently reported on in-line multi step CIGSe [11] absorbers. ALD-In<sub>2</sub>S<sub>3</sub> has an uncertified record efficiency of 16.4 % [7], also on pure selenide absorbers. This means that the value of 16.1% presented in this paper is, to our knowledge, the best independently confirmed efficiency for devices with an In<sub>2</sub>S<sub>3</sub> buffer layer. In this paper we present an optimized deposition process for Spray ILGAR and the corresponding increase in the performance of the devices and compare them with the previous record cell.

## EXPERIMENTAL

The spray-ILGAR method is a sequential and cyclic technique that enables the deposition of thin film layers on suitable absorbers. During a cycle, an alcoholic solution containing the metal precursor is first sprayed on the heated substrate by means of aerosol assisted chemical vapor deposition (AA-CVD) at atmospheric pressure and then sulfurized by a reactive gas. This cycle is repeated until the desired thickness is reached. A full description of the process can be found elsewhere [12].

For the preparation of the buffer layers in this work, an ethanol solution containing either  $\text{InCl}_3$  or  $\text{In}(\text{acac})_3$  (acac = acetylacetonate) is sprayed onto commercially available CIGSSe absorbers cut down to a size of  $2.5 \times 2.5 \text{ cm}^2$ . The chlorine content of the buffer layers is varied by changing the metal precursor and/or the deposition conditions such as the  $\text{H}_2\text{S}$  concentration and the spraying and sulfurization times. For some experiments water is added to the solution, which results in an increased deposition rate.  $\text{N}_2$  is used as a carrier gas, with a flow rate of 5.5 l/min. The density of the aerosol is externally controlled using a laser and a photodetector. During the spraying phase, the transmitted laser light intensity is kept at 50% of the initial (maximum) value to ensure a reproducible spraying step throughout the process and for different samples. During the sulfurization step, 100 %  $\text{H}_2\text{S}$  is used as a reactive gas, with a flow rate of approximately 0.95 l/min, and it is mixed with the carrier gas. All the absorbers were provided by BOSCH CISTech Solar GmbH and show the usual stacked layers: glass, molybdenum and CIGSSe. The absorber layer is formed by DC sputtering of the Cu-Ga-In precursor followed by a chalcogenization in a furnace. More details can be found elsewhere [13]. All samples belonging to the same run or experiment are cut from the same absorber plate in order to ensure relevant and comparable results. In the present work we have tuned the spray-ILGAR deposition process for  $\text{In}_2\text{S}_3$  buffer layers by changing the metal precursor, the  $\text{H}_2\text{S}$  flow rate (and therefore the  $\text{H}_2\text{S}$  concentration) in the sulfurization step as well as the amount of water added to the alcoholic solution. Absorbers in format  $5 \times 5 \text{ cm}^2$  have been prepared in parallel with a CdS buffer layer by CBD for comparison. All solar cells have been completed by a sputtered i-ZnO/ZnO:Al window bilayer and evaporated Ni-Al contact grids for better current collection. Each  $2.5 \times 2.5 \text{ cm}^2$  sample ( $5 \times 5 \text{ cm}^2$  in case of the CdS-buffered references) has been divided into eight (thirty-two)  $0.5 \text{ cm}^2$  solar cells. The electrical characterization has been done using an in-house class A sun simulator calibrated using a silicon solar cell as a reference under standard test conditions (AM 1.5 G,  $100 \text{ mW/cm}^2$  and  $25 \text{ }^\circ\text{C}$ ). The current densities and efficiencies presented in this work are calculated using the total area i.e. the area covered by the grids is also considered for the current density and efficiency calculations. Quantum efficiency analysis has been performed using an illumination system including two sources (halogen and xenon lamps) and a

Bentham TM300 monochromator. Reference measurements are done on calibrated Si and Ge detectors. Two high efficiency solar cells have been sent to the Fraunhofer Institut für Solare Energiesysteme (ISE) for certification. These measurements took place two to three weeks after the completion of the cells. Similar high efficiency cells were measured weekly at our in-house system to account for possible degradation. These measurements are all performed in our in-house system which inhibits a lower experimental accuracy than the ISE Fraunhofer certification. Especially the short circuit current density is expected to have an absolute error of approximately +/- 5%. Relative values for one experimental series are however accurate. In addition,  $\text{In}_2\text{S}_3$  films have been analyzed by scanning electron microscopy (SEM) and x-ray fluorescence (XRF) to determine their thickness and composition. For SEM a LEO-GEMINI field emission gun microscope has been used, with an in-lens detector and a point resolution of 1nm. XRF has been performed using a Philips MagiX Pro wavelength dispersive X-ray fluorescence spectrometer with Rh  $\text{K}\alpha$  radiation. The calibration of the XRF has been performed by means of elastic recoil detection analysis (ERDA) measurements on similar layers deposited on freshly etched silicon substrates. To determine the band gap of the ILGAR- $\text{In}_2\text{S}_3$  layers on quartz substrate, transmission and reflection spectra have been measured with an optical Cary 500 spectrometer with an integration sphere. Evaporated  $\text{In}_2\text{S}_3$  buffer layers are deposited onto the same absorbers by thermal evaporation (or physical vapor deposition, PVD). In this case, compound  $\text{In}_2\text{S}_3$  powder is taken as source material and evaporated from a crucible at a temperature of 720°C onto the substrate, which is not actively heated and therefore stays at temperatures below 40°C. The thickness of the evaporated buffer layers is approximately 40-50nm. For more details on this technique, the reader is referred to reference [10].

## RESULTS AND DISCUSSION

When working with Cl-containing indium precursors, the sulfurization step is critical to control how much chlorine remains unreacted in the layer. The efficiency of the ILGAR-  $\text{In}_2\text{S}_3$  buffered CIGS<sub>Se</sub> solar cells shows a clear trend as a function of the chlorine content in the buffer layer. Chlorine-free layers can be easily obtained from Cl-free precursors. The amount of chlorine in a layer grown using a Cl-containing precursor can be varied by the choice of precursors and by changing the sulfurization step, in terms of  $\text{H}_2\text{S}$  flow rate (concentration) and step duration. Whereas the short circuit current density ( $J_{sc}$ ) is nearly independent of the Cl-content (up to 22 at% chlorine), the fill factor (FF) shows a decrease with increasing Cl-content and the open circuit voltage ( $V_{oc}$ ) has a maximum for Cl-free layers. It must be noted that Cl-free layers have been obtained from  $\text{In}(\text{acac})_3$  instead of using  $\text{InCl}_3$ , and it is not clear yet whether the increased voltage is a result of the absence of

chlorine in the layer or of the alternative indium precursor used in the solution which may lead to a different growth mechanism.

The increased voltage can be a consequence of a change in the density and energy position of defect states associated with the interface affecting both the charge and carrier recombination, although the nature of the interface as a function of the chlorine content remains a topic for further investigation. Figure 1 shows the photovoltaic parameters (average and value of the cell with the highest efficiency) of the measured samples. For each experimental condition two 2.5x2.5 cm<sup>2</sup> samples have been prepared, each containing eight solar cells (0.5 cm<sup>2</sup> total area). The average values are calculated from the best six cells from the total eight.

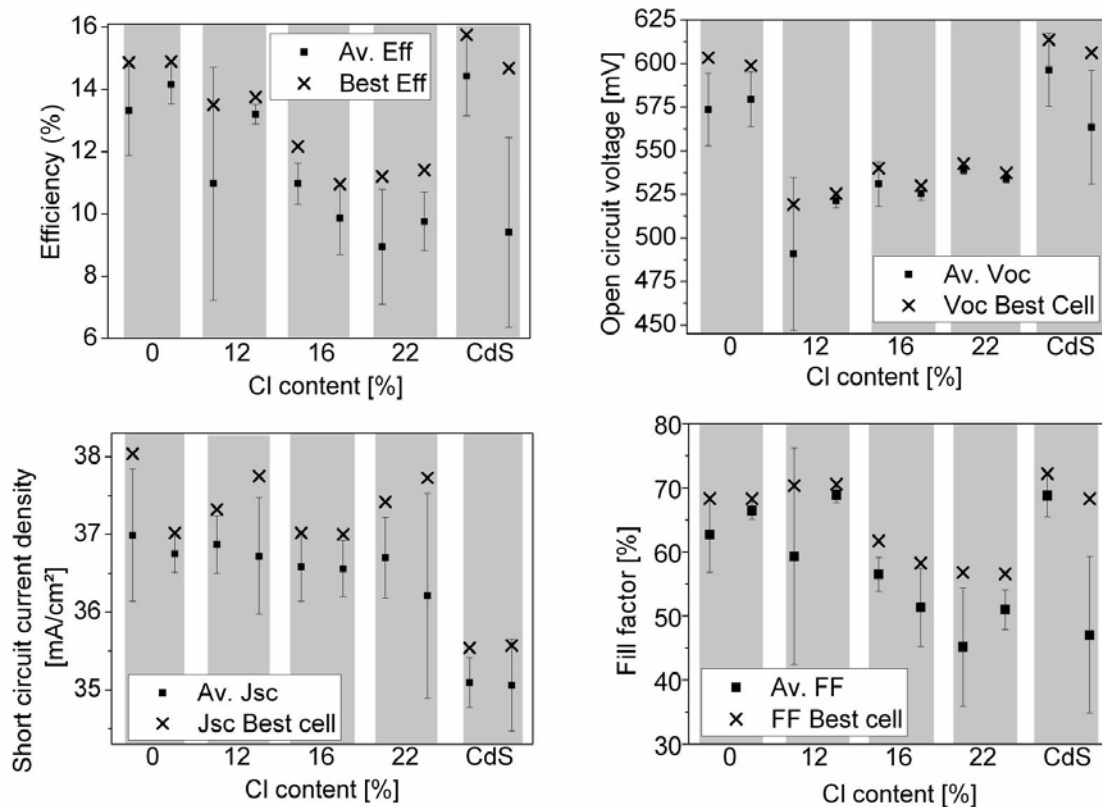


Figure 1. Photovoltaic parameters of Spray-ILGAR In<sub>2</sub>S<sub>3</sub>/CIGSSe cells as a function of the chlorine content of the buffer layer. All average values (solid squares) are taken as the mean of the best six cells from eight (75 % of the total number of cells). The crosses indicate the corresponding parameter of the most efficient, and not the best value. Bars represent the standard deviation.

Once the optimum chlorine content for the CIGSSe absorbers under study has been found, namely no chlorine, the H<sub>2</sub>S flow during the sulfurization has been varied. Figure 2 shows the average (solid squares) and best (crosses) efficiency as a function of the H<sub>2</sub>S flow. Here again, two samples have been prepared for each experimental condition.

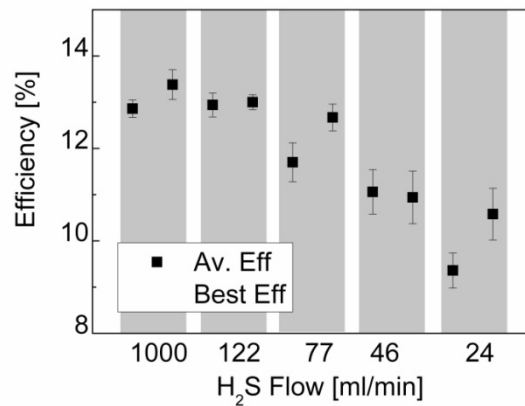


Figure 2. Efficiencies of Spray-ILGAR In<sub>2</sub>S<sub>3</sub>/CIGSSe cells as a function of the H<sub>2</sub>S flow during the sulfurization step. All average values are taken as the mean of the best six cells from eight (75 % of the total number of cells). Bars represent the standard deviation.

Good working cells can be achieved using H<sub>2</sub>S flow rates as low as 77 ml/min, but the performance decreases for lower flow rates as a consequence of an incomplete sulfurization reaction of the precursor layer deposited during the spray step, which results in an In(O,OH,C,S) rather than in the desired In<sub>2</sub>S<sub>3</sub> layer.

With the knowledge of the optimal chlorine content of the In<sub>2</sub>S<sub>3</sub> layers and the optimal H<sub>2</sub>S flow, three sets of chlorine-free samples have been prepared using In(acac)<sub>3</sub> precursors with different purities, with different concentrations, temperature and number of cycles. In some cases 1% of water has been added. The sulfurization step has been carried out using a H<sub>2</sub>S flow rate of ~1000 ml/min. The recipes used for each run are shown in table 1.

Table 1. Experimental conditions of the different sets of samples. Runs A–C consist of ILGAR-In<sub>2</sub>S<sub>3</sub> buffered CIGSSe absorbers. Run D is the corresponding CdS reference made with CIGSSe absorbers from the same batch.

Run	# cells	Precursor	Water	Concentration	Temperature	# Cycles
A	72	In(acac) <sub>3</sub> 99%	1%	30 mM	225 °C	5
B	32	In(acac) <sub>3</sub> 99%	1%	25 mM	175 °C	9
C	48	In(acac) <sub>3</sub> 98%	0%	25 mM	225 °C	6
D	38	CdS Reference	N. A.	N. A.	N. A.	N. A.

Figure 3 shows the efficiency frequency of all runs, including the CdS references. The cells with the highest conversion efficiencies (16.8 % and 16.5 %, in house measurements) were sent to the Fraunhofer ISE for independent confirmation, while a sample from each run was measured every week to exclude a possible degradation of the performance with time.

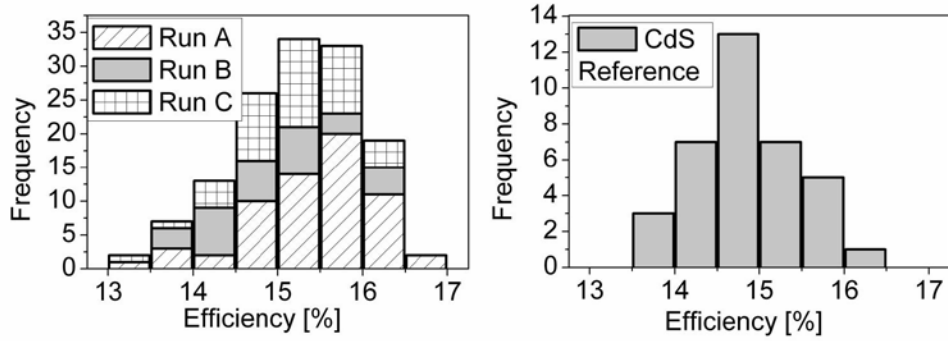


Figure 3. Distribution of cell efficiencies of the different runs processed with  $\text{In}_2\text{S}_3$  (left) and the distribution of cell efficiencies of the CdS-buffered references (right). The recipes used for each run can be found in table 1.

Table 2 shows the average and standard deviations of the PV parameters of the corresponding runs. For the calculation, cells with low efficiencies due to short circuiting or damage have not been taken into account. The number of the excluded cells is 8 out of 72 for Run A, 2 out of 32 for run B and 5 out of 48 for run C. For CdS References, 37 out of 38 cells have been used for the calculation. In the case of the  $\text{In}_2\text{S}_3$  buffered samples ( $2.5 \times 2.5 \text{ cm}^2$ ) all eight cells are located at the border of the sample, which may account for the increased number of damaged cells compared to  $5 \times 5 \text{ cm}^2$  CdS-references, where all measured cells were located in the center of the sample, at least 0.5 cm away from the edge. All three  $\text{In}_2\text{S}_3$  recipes result in devices with higher average efficiencies than the CdS-buffered references, mostly due to an increased open circuit voltage.

Table 2: Average photovoltaic parameters and corresponding standard deviations of the cells processed in runs A-D, being D the CdS-buffered references.

Run	# valid cells	Av. Eff (%)	Av. Voc (mV)	Av. FF (%)	Av. Jsc( $\text{mA}/\text{cm}^2$ )
A	64/72	$15.4 \pm 0.7$	$628 \pm 6$	$69.6 \pm 1.9$	$35.3 \pm 0.9$
B	30/32	$14.9 \pm 0.8$	$630 \pm 8$	$67.4 \pm 2.0$	$35.5 \pm 0.9$
C	43/48	$15.1 \pm 0.7$	$624 \pm 9$	$68.2 \pm 2.0$	$35.7 \pm 0.6$
D (CdS)	37/38	$14.7 \pm 0.6$	$599 \pm 7$	$69.8 \pm 1.9$	$35.3 \pm 1.0$

The cells sent to the Fraunhofer ISE for certification have been measured two to three weeks after preparation and are located in two different samples processed in Run A. The certified current-voltage curves are shown in figure 4 (left). Both solar cells have an efficiency of 16.1%. This is, to our knowledge, the highest certified efficiency for solar cells with an  $\text{In}_2\text{S}_3$  buffer layer. The slightly higher efficiencies of the in-house measurement when compared to the certified results can be due to an overestimated short-circuit current ( $V_{oc}$  and FF show very similar values), or to a degradation of the performance with time. The efficiency values

of a comparable sample after one, two, three and four weeks are also shown in figure 4 (right). There is a slight trend towards lower efficiencies after the third week. Since the certified solar cells were measured between the second and the third week, no clear sign of degradation is found.

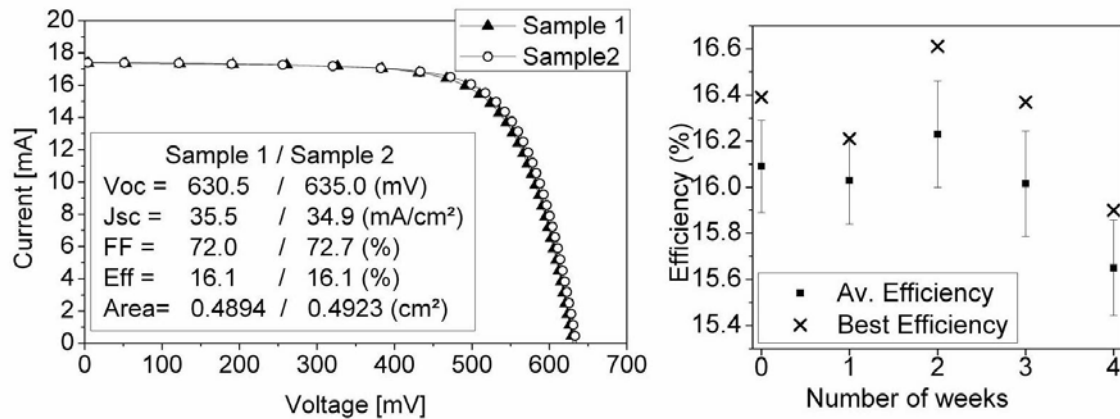


Figure 4: Mo/CIGSSe/ILGAR-In<sub>2</sub>S<sub>3</sub>/ZnO certified current-voltage characteristics (left). Average and best efficiencies of a twin sample buffered using the same conditions and measured weekly. Bars represent the standard deviation. Certification took place between two and three weeks after the first in-house measurement.

If these values are compared with those of the previous ILGAR-In<sub>2</sub>S<sub>3</sub> record cell [9] (see table 3) a clear difference is observed. The previous record on commercially available absorber from AVANCIS GmbH & Co. KG, with 14.7 % conversion efficiency, had a higher short circuit current but a lower open circuit voltage than the corresponding CdS reference. This cell was buffered with In<sub>2</sub>S<sub>3</sub> using InCl<sub>3</sub> as a precursor and the corresponding chlorine content was measured to be around 12 at% with XRF.

Table 3. Photovoltaic parameters of In<sub>2</sub>S<sub>3</sub>-buffered CIGSSe cells certified in the given years and the corresponding approximate thickness (d), band gap (E<sub>g</sub>) and chlorine content ([Cl]) of the buffer layers.

Year	d [nm]	E <sub>g</sub> [eV]	[Cl] (at%)	V <sub>oc</sub> (mV)	J <sub>sc</sub> (mA/cm <sup>2</sup> )	FF (%)	η (%)
2005	23	2.4	12%	574	37.4	68.4	14.7
2011	35	2.0	0%	631	35.5	72	16.1

When comparing the quantum efficiencies of the In<sub>2</sub>S<sub>3</sub> record cells (with and without chlorine) with the corresponding CdS reference, as shown in figure 5, the expected gain in the blue wavelength region is not seen for the Cl-free sample. This gain is clear in the case of the Cl-containing CIGSSe/In<sub>2</sub>S<sub>3</sub> device. The increased absorption in the blue wavelength region can

be attributed to two facts. On one hand,  $\text{In}_x\text{S}_y\text{Cl}_z$  shows a larger band gap (indirect) for higher chlorine contents. Figure 6 shows the  $(h\nu\alpha)^{1/2}$  vs. energy plots of two glass samples coated with  $\text{In}_2\text{S}_3$  with different chlorine contents as well as the extrapolated lines used to determine the band gap. The chlorine free sample shows a band gap of  $\sim 2.0$  eV, whereas a layer containing 14 at% chlorine, and being therefore similar to the 12 at% of the record cell from 2005, has a band gap of approximately 2.4 eV. On the other hand, the Cl-free buffer layer is thicker. The previous record cell included a buffer layer with a thickness of  $\sim 23$  nm, extrapolated from a thick sample measured by means of XRF, which resulted in a growth rate of  $\sim 3.3$  nm/cycle. In the case of the 16.1 % efficiency sample, the thickness has been estimated from similar samples analyzed by means of SEM (on a Mo/ $\text{In}_2\text{S}_3$  system) and XRF (on a glass/ $\text{In}_2\text{S}_3$  system). The resulting thickness is estimated to be  $35 \pm 5$  nm, approximately 50% thicker than in the previous record cell.

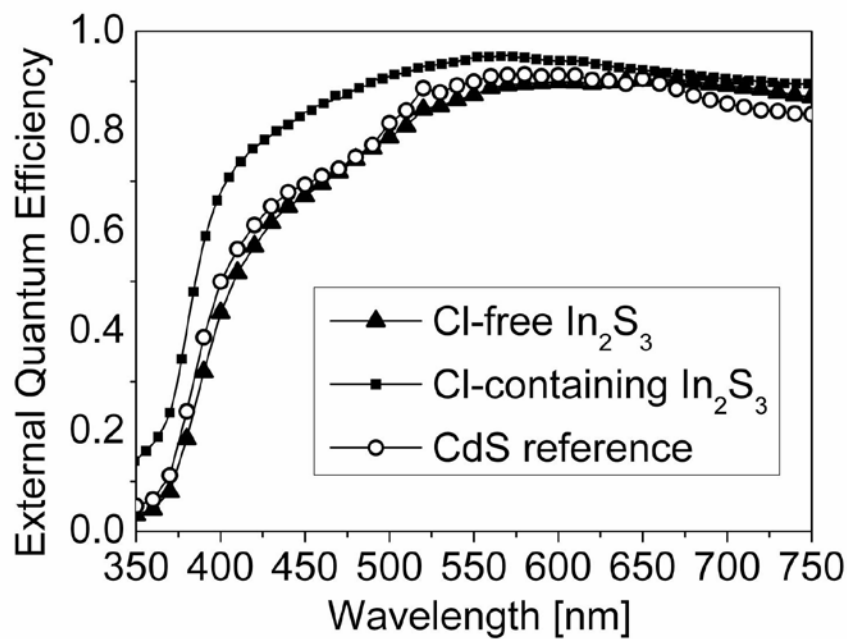


Figure 5: Short wavelength region of the external quantum efficiencies of CIGSSe devices with a Cl-free ILGAR  $\text{In}_2\text{S}_3$ , a Cl-containing ILGAR- $\text{In}_2\text{S}_3$  and a CdS buffer layer.



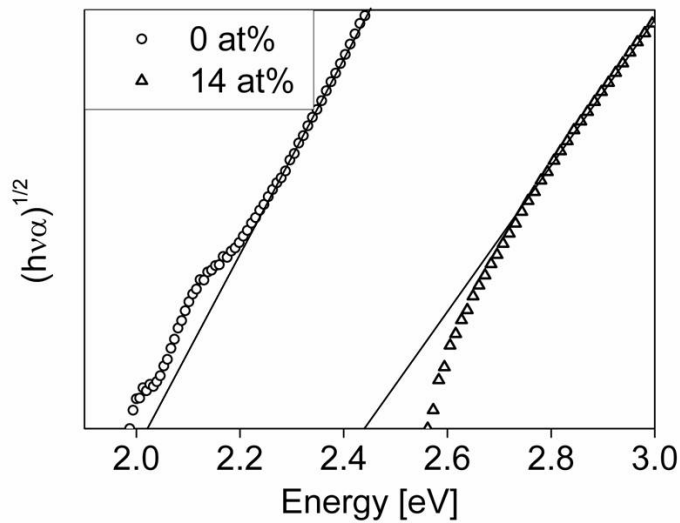


Figure 6. Fitted  $(h\nu\alpha)^{1/2}$  vs. Energy curves used to determine the optical band gap of the  $\text{In}_2\text{S}_3$  layers. The band gaps are  $\sim 2.0$  eV for the Cl-free layer and  $\sim 2.4$  eV for the layer with 14.5 at% chlorine

The Cl content in the  $\text{In}_2\text{S}_3$  buffer layer has been found to have a significant effect on solar cell parameters also for devices with an evaporated  $\text{In}_2\text{S}_3$  buffer layer. If an  $\text{In}_2\text{S}_3$  buffer is deposited onto the same absorbers by this technique the presence of Cl in the buffer layer has an interesting influence on cell performance and especially the annealing behavior of the devices. Samples with evaporated  $\text{In}_2\text{S}_3$  layer generally need a thermal annealing step at  $200^\circ\text{C}$  in air after completing the devices with the ZnO window for an optimal performance. In the case of ILGAR buffers this annealing step is not necessary because the deposition already takes place at  $175\text{--}225^\circ\text{C}$ . Figure 7 shows the development of the average cell efficiency (Sample PVD A, left) and cell parameters (right) upon annealing at  $200^\circ\text{C}$  for a typical sample of this kind. The average efficiency starts in the as grown state at a value as low as  $(9.3\pm 0.4)\%$  and gradually increases upon annealing to  $(13.9\pm 0.4)$  after 45min, due to an increase in both, fill factor and open circuit voltage.

If a commercial  $\text{In}_2\text{S}_3$  powder with a significant incorporation of  $\text{InCl}_3$  (several atomic %, probably due to an incomplete sulfurization during the synthesis) is used as source material, the annealing behavior is completely different (figure 7 left, Sample PVD B). In this case the  $\text{InCl}_3$  incorporated in the source material already starts evaporating at much lower temperatures ( $> 420^\circ\text{C}$ ) and therefore in the first deposition from this kind of source material nearly all residual  $\text{InCl}_3$  is deposited onto the absorber prior to the  $\text{In}_2\text{S}_3$  deposition. For the resulting devices with a  $\text{InCl}_3/\text{In}_2\text{S}_3$  buffer layer system, the average efficiency in the as grown state shows high efficiencies of above 13%. However, it does not increase further during annealing as in the case of the pure  $\text{In}_2\text{S}_3$  layers. To the contrary, the open circuit voltage decreases during annealing by approximately 30mV showing values lower than

those of the annealed Cl-free devices. The current, on the other hand, is slightly higher in the case of devices with Cl-containing evaporated  $\text{In}_2\text{S}_3$  buffer layers, as it is in the case of ILGAR.

It is known that a strong Cu diffusion into the  $\text{In}_2\text{S}_3$  takes place at temperatures above  $200^\circ\text{C}$ , which could be independently demonstrated during the deposition of Spray-ILGAR  $\text{In}_2\text{S}_3$  [14] and during the annealing of devices with PVD  $\text{In}_2\text{S}_3$  [15]. One hypothesis for the altered annealing behavior is that an increasing Cl content influences the Cu diffusion into the  $\text{In}_2\text{S}_3$  which is beneficial for an optimum cell performance

While the reasons for this behavior should still be further investigated, it seems clear that a chlorine-free or at least low-chlorine absorber/buffer interface gives best performance results in most cases. As further examples, the use of  $\text{ZnS}/\text{In}_2\text{S}_3$  bilayers [16] or  $\text{ZnS}$  nanodot passivation layer / point contact buffer films [17] can be regarded as systems where this effect is also encountered. In both cases, the  $\text{ZnS}$  is grown from Cl-free precursors.

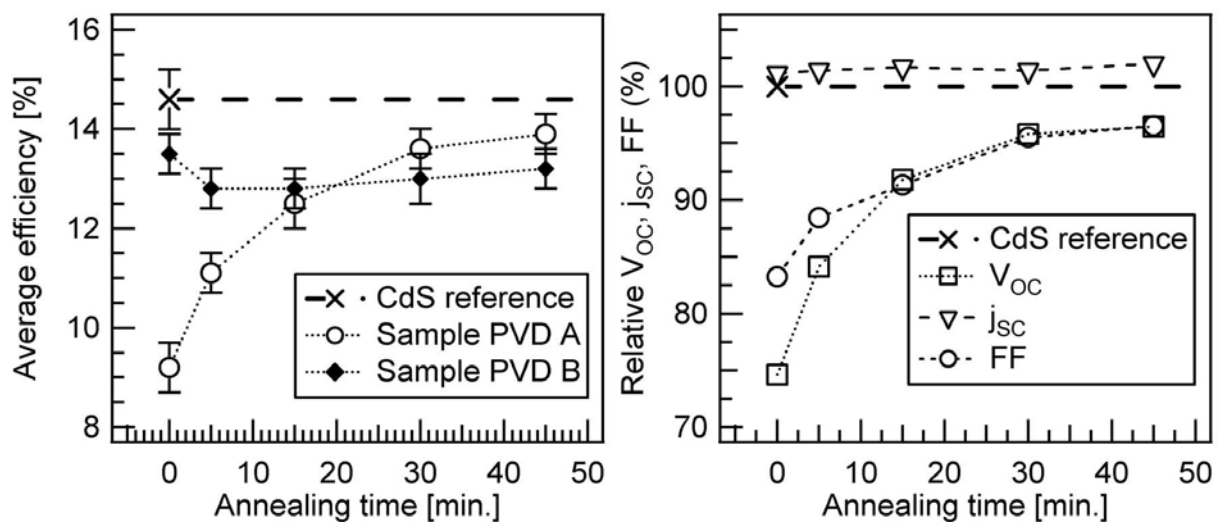


Figure 7. (left) Efficiencies of two samples with thermally evaporated  $\text{In}_2\text{S}_3$  buffer layer from different source materials: Sample PVD A: pure  $\text{In}_2\text{S}_3$ . Sample PVD B:  $\text{In}_2\text{S}_3$  with traces of  $\text{InCl}_3$ . Shown is the development of the average efficiency (16 cells per sample) after several, subsequent annealing steps at  $200^\circ\text{C}$  in air. The average efficiency of a CBD CdS sample (not annealed) is added for reference. (right) Development of the average cell parameters  $V_{OC}$ ,  $j_{SC}$  and fill factor of sample A relative to corresponding values for the CdS reference ( $\eta$ :  $(14.6 \pm 0.6)\%$ ,  $V_{OC}$ :  $(605 \pm 8)\text{mV}$ ,  $j_{SC}$ :  $(35.0 \pm 0.4)\text{mA}/\text{cm}^2$ , FF:  $(69.2 \pm 1.8)\%$ ). Bars represent the standard deviation.

## CONCLUSION

In this work we have demonstrated, based on a large statistical study, that CIGSSe solar cells with an ILGAR  $\text{In}_2\text{S}_3$ -buffer layers can reach higher efficiencies than the corresponding

CdS references if proper deposition conditions are met. The higher efficiencies are due to an increased open circuit voltage that not only matches that of CdS-buffered devices but surpasses it by approximately 30 mV. The increase in the open circuit voltage has been obtained by a fine tuning of the chlorine content of the buffer layer and the sulfurization step. A similar behavior is also observed in cells with an evaporated  $\text{In}_2\text{S}_3$  buffer layer. Devices with an  $\text{In}_2\text{S}_3$  buffer layer with efficiencies above 16 % have been independently confirmed for the first time by the Fraunhofer ISE. These cells have no antireflective coating and the TCO thickness has not yet been optimized to obtain a higher collection current. Furthermore, these high efficiencies have been obtained by buffering commercially available CIGSSe absorber with a non toxic material deposited by a quasi-dry and vacuum-free process, which up-scaling up to  $30 \times 30 \text{ cm}^2$  in an in-line prototype coater has been already demonstrated.

## ACKNOWLEDGEMENTS

The authors would like to thank Michael Kirsch and Carola Kelch for the completion of the devices and the CdS references. This work is part of the NeuMaS project founded by the German Federal Ministry of Education and Research.

## REFERENCES

- [1] Jackson P, Hariskos D, Lotter E, Paetel S, Würz R, Menner R, Wischmann W, Powalla M. New world record efficiency for  $\text{Cu}(\text{In,Ga})\text{Se}_2$  thin film solar cells beyond 20%. *Progress in Photovoltaics: Research and Applications* 2011; **19**: 894-897
- [2] Green MA, Emery K, Hishikawa Y, Warta W. Solar cell efficiency tables (version 37). *Progress in Photovoltaics: Research and Applications* 2011; **19**: 84-92
- [3] Dalibor T, Jost S, Vogt H, Heiß A, Visbeck S, Happ T, Palm J, Avellán A, Niesen T, Karg F. Towards module efficiencies of 16% with an improved CIGSSe device design. *Proceedings of the 26<sup>th</sup> European Photovoltaic Solar Energy Conference and Exhibition*. WIP: Munich, 2011; 2407-2411
- [4] Naghavi N, Abou-Ras D, Allsop N, Barreau N, Bücheler S, Ennaoui A, Fischer CH, Guillen C, Hariskos D, Herrero J, Klenk R, Kushyia K, Lincot D, Menner R, Nakada T, Platzer-Björkman C, Spiering S, Tiwari AN, Törndahl T. Buffer layers and transparent conducting oxides for chalcopyrite  $\text{Cu}(\text{In,Ga})(\text{S,Se})_2$  based thin film photovoltaics: present status and current developments. *Progress in Photovoltaics: Research and Applications* 2010; **18**: 441
- [5] Strohm A, Eisenmann L, Gebhardt RK, Harding A, Schlötzer T, Abou Ras D, Schock HW.  $\text{ZnO}/\text{In}_x\text{S}_y/\text{Cu}(\text{In,Ga})\text{Se}_2$  solar cells fabricated by coherent heterojunction formation. *Thin Solid Films* 2005; **480-481**: 162-167
- [6] Grimm A, Kieven D, Klenk R, Laueremann I, Neisser A, Niesen T, Palm J. Junction formation in chalcopyrite solar cells by sputtered wide gap compound semiconductors. *Thin Solid Films* 2011; **520**: 1330-1333
- [7] Naghavi N, Spiering S, Powalla M, Cavanna B, Lincot D. High-efficiency copper indium gallium diselenide (CIGS) solar cells with indium sulphide buffer layers deposited by atomic layer chemical vapor deposition (ALCVD). *Progress in Photovoltaics: Research and Applications*. 2003; **11**: 437-443

- [8] Allsop NA, Schönmann A, Belaidi A, Muffler HJ, Metersacker B, Bohne W, Strub E, Röhlich J, Lux-Steiner MC, Fischer CH. Indium sulfide thin films deposited by the spray ion layer gas reaction technique. *Thin solid films* 2006; **13**: 52-56
- [9] Allsop N, Schönmann A, Muffler HJ, Bär M, Lux-Steiner MC, Fischer CH. Spray-ILGAR indium sulfide buffers for Cu(In,Ga)(S,Se)<sub>2</sub> solar cells. *Prog. Photovoltaics: Res. Appl.* 2005; **13**: 607–616
- [10] Spiering S, Kessler F, Wischmann W. Indium sulphide buffer layers by in-line evaporation for CIGS thin film devices. *Proceedings of the 26<sup>th</sup> European Photovoltaic Solar Energy Conference and Exhibition*. WIP: Munich, 2011; 2886-2889.
- [11] Pistor P, Caballero R, Hariskos D, Izquierdo-Roca V, Wächter R, Schorr S, Klenk K. Quality and stability of compound indium sulphide as source material for buffer layers in Cu(In,Ga)Se<sub>2</sub> solar cells. *Solar Energy Materials & Solar cells* 2009; **93**: 148-152
- [12] Fischer CH, Allsop N, Gledhill SE, Köhler T, Krüger M, Sáez-Araoz R, Fu Y, Schwieger R, Richter J, Wohlfart P, Bartsch P, Lichtenberg N, Lux-Steiner MC. The Spray-ILGAR (ion layer gas reaction) method for the deposition of thin semiconductor layers: Process and applications for thin film solar cells. *Solar Energy Materials & Solar cells* 2011; **95**: 1518-1526
- [13] Probst V, Hergert F, Walther B, Thyen R, Batereau-Neumann G, Neumann B, Windeck A, Letzig T, Gerlach A. High Performance CIS Solar modules: Status of production and development at Johanna Solar Technology. *Proceedings of the 24<sup>th</sup> European Photovoltaic Solar Energy Conference and Exhibition*. WIP: Munich, 2009; 2455-2459
- [14] Bär M, Allsop N, Lauermann I, Fischer, Ch.-H. Deposition of In<sub>2</sub>S<sub>3</sub> on Cu(In,Ga)(S,Se)<sub>2</sub> thin film solar cell absorbers by ion layer gas reaction: evidence of strong interfacial diffusion. *Applied Physics Letters* 2007; **90**: 132118
- [15] Pistor P, Allsop N, Braun W, Caballero R, Camus C, Fischer C.-H, Gorgoi M, Grimm A, Johnson B, Kropp T, Lauermann I, Lehmann S, Mönig H, Schorr S, Weber A, Klenk R. Cu in In<sub>2</sub>S<sub>3</sub>: interdiffusion phenomena analysed by high kinetic energy X-ray photoelectron spectroscopy. *Physica Status Solidi A* 2009; **206**: 1059-62
- [16] Allsop N, Camus C, Hänsel A, Gledhill SE, Lauermann I, Lux-Steiner MC, Fischer CH. Indium sulfide buffer/CIGSSe interface engineering: Improved cell performance by the addition of zinc sulfide. *Thin Solid Films* 2007; **515**: 6068-6072
- [17] Fu Y, Allsop N, Gledhill SE, Köhler T, Krüger M, Sáez-Araoz R, Blöck U, Lux-Steiner MC, Fischer CH. ZnS nanodot film as defect passivation layer for Cu(In,Ga)(S,Se)<sub>2</sub> thin-film solar cells deposited by Spray-ILGAR (Ion-Layer Gas Reaction). *Advanced energy materials* 2011; **1**: 561-564  
DOI:10.1002/aenm.201100146